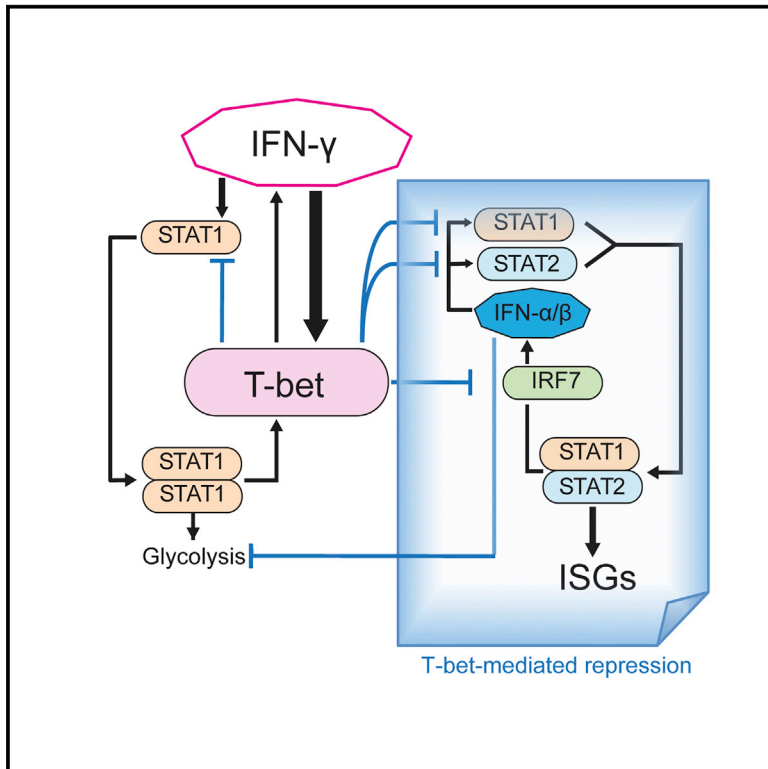


Immunity

The Transcription Factor T-bet Limits Amplification of Type I IFN Transcriptome and Circuitry in T Helper 1 Cells

Graphical Abstract



Authors

Shigeru Iwata, Yohei Mikami,
Hong-Wei Sun, ..., John J. O'Shea,
Fred P. Davis, Yuka Kanno

Correspondence

john.oshea@nih.gov (J.J.O.),
fred.davis@nih.gov (F.P.D.),
kannoy@mail.nih.gov (Y.K.)

In Brief

T-bet directs T helper 1 cell differentiation and IFN-γ production. Iwata et al. find that T-bet also acts as a repressor of type I IFN transcription factors and type-I-IFN-stimulated genes and collectively restrains IFN-γ-induced collateral type I IFN circuitry during the Th1 response.

Highlights

- T-bet-repressed genes are enriched with type-I-IFN-stimulated genes (ISGs)
- T-bet constrains activity of type I IFN transcription factors in IFN-γ conditions
- Blocking IFNAR rectifies aberrant ISG expression by IFN-γ in T-bet knockout cells
- T-bet restrains IFN-γ-induced collateral type I IFN circuitry in the Th1 response in vivo

The Transcription Factor T-bet Limits Amplification of Type I IFN Transcriptome and Circuitry in T Helper 1 Cells

Shigeru Iwata,^{1,8,9} Yohei Mikami,^{1,8} Hong-Wei Sun,² Stephen R. Brooks,² Dragana Jankovic,³ Kiyoshi Hirahara,⁴ Atsushi Onodera,^{4,5} Han-Yu Shih,¹ Takeshi Kawabe,^{3,7} Kan Jiang,¹ Toshinori Nakayama,^{4,6} Alan Sher,³ John J. O'Shea,^{1,*} Fred P. Davis,^{1,*} and Yuka Kanno^{1,10,*}

¹Molecular Immunology and Inflammation Branch

²Biodata Mining and Discovery Section

National Institute of Arthritis and Musculoskeletal and Skin Diseases, National Institutes of Health, Bethesda, MD 20892, USA

³Immunobiology Section, Laboratory of Parasitic Diseases, National Institute of Allergy and Infectious Diseases, National Institutes of Health, Bethesda, MD 20892, USA

⁴Department of Immunology, Graduate School of Medicine, Chiba University, Chiba 260-8670, Japan

⁵Institute for Global Prominent Research, Chiba University, Chiba 260-8670, Japan

⁶AMED-CREST, AMED, Chiba 260-8670, Japan

⁷Cytokine Biology Unit, Laboratory of Immunology, National Institute of Allergy and Infectious Diseases, National Institutes of Health, Bethesda, MD 20892, USA

⁸These authors contributed equally

⁹Present address: First Department of Internal Medicine, University of Occupational & Environmental Health, Kitakyushu 807-8555, Japan

¹⁰Lead Contact

*Correspondence: john.oshea@nih.gov (J.J.O.), fred.davis@nih.gov (F.P.D.), kannoy@mail.nih.gov (Y.K.)

<http://dx.doi.org/10.1016/j.immuni.2017.05.005>

SUMMARY

Host defense requires the specification of CD4⁺ helper T (Th) cells into distinct fates, including Th1 cells that preferentially produce interferon- γ (IFN- γ). IFN- γ , a member of a large family of anti-pathogenic and anti-tumor IFNs, induces T-bet, a lineage-defining transcription factor for Th1 cells, which in turn supports IFN- γ production in a feed-forward manner. Herein, we show that a cell-intrinsic role of T-bet influences how T cells perceive their secreted product in the environment. In the absence of T-bet, IFN- γ aberrantly induced a type I IFN transcriptomic program. T-bet preferentially repressed genes and pathways ordinarily activated by type I IFNs to ensure that its transcriptional response did not evoke an aberrant amplification of type I IFN signaling circuitry, otherwise triggered by its own product. Thus, in addition to promoting Th1 effector commitment, T-bet acts as a repressor in differentiated Th1 cells to prevent aberrant autocrine type I IFN and downstream signaling.

INTRODUCTION

Proper response to diverse microbial pathogens requires that CD4⁺ helper T cells acquire distinct fates manifested by their ability to selectively produce cytokines to appropriately respond to these different infectious challenges (Zhu et al.,

2010). T helper 1 (Th1) cells and their product IFN- γ (type II IFN) are essential for resistance to pathogens, especially intracellular bacteria and parasites (Dunn et al., 2006; Sallusto, 2016; Zhu et al., 2010). In contrast, type I IFNs, a large family of related proteins including IFN- α and IFN- β , are produced by many cell types and induce interferon-stimulated genes (ISGs), which mediate protective responses, especially against viruses (Mostafavi et al., 2016; Schneider et al., 2014; Theofilopoulos et al., 2005). Despite their names, the actions of IFN- γ and type I IFNs are generally thought to be quite distinct, consistent with the differential patterns of response required for the types of infection (Boehm et al., 1997; Schneider et al., 2014).

Specification of distinct fates for T cells represents an integration of environmental and cytokine signals through signal-dependent transcription factors (SDTFs) and the action of intrinsic lineage-defining transcription factors (LDTFs) (Heinz et al., 2015). For Th1 cells, T-bet (encoded by *Tbx21*) is the recognized LDTF and mediates direct, positive feed-forward regulation of IFN- γ production (Szabo et al., 2000). For Th1 cells to maintain cellular fitness and proliferative capacity while producing their signature cytokine, Th1 cells need to adapt to the local cellular environment they create, i.e., a high level of IFN- γ (Yosef and Regev, 2016). As opposed to an SDTF, such as STAT1, which is directly activated by IFN- γ to induce transactivation of targets, the role of an LDTF such as T-bet in IFN- γ signaling has not been fully addressed. With genomic approaches, we explored the actions of T-bet beyond its recognized roles in promoting Th1 cell differentiation. We found that T-bet activated and repressed equal fractions of genes in T cells treated with IFN- γ , but an unexpected broad action of T-bet as a repressor was to restrain aberrant type I IFN circuitry in Th1 cells.

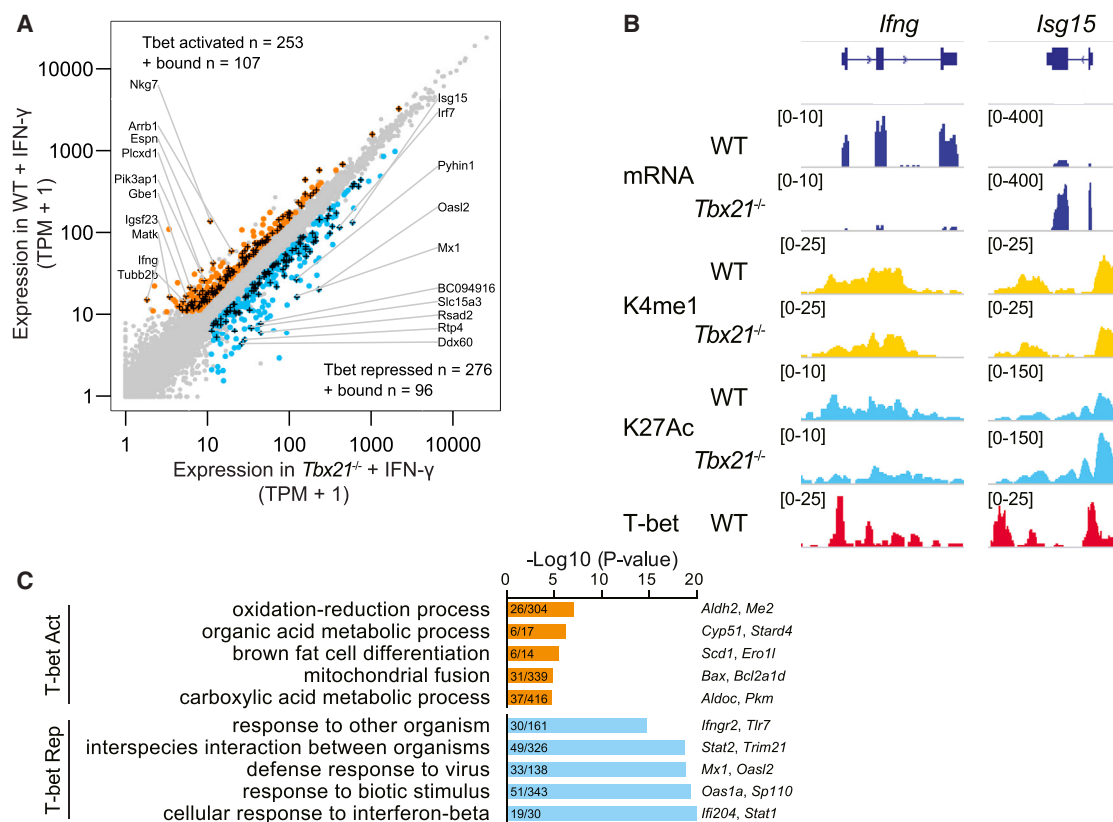


Figure 1. T-bet Represses Type I IFN Signature Genes in IFN- γ -Exposed CD4 T Cells

Naive T cells were activated by CD3⁺CD28⁺ IFN- γ (100 ng/ml) for 3 days and subjected to mRNA-seq and ChIP-seq (T-bet, H3K4me1, and H3K27Ac).

(A) Direct T-bet targets are both positively and negatively regulated by T-bet. A scatterplot of gene expression by RNA-seq compares wild-type (WT) and *Tbx21*^{-/-} CD4⁺ T cells. mRNA-seq (n = 3 per genotype) was used to identify differentially expressed genes with the sleuth R package with a cutoff q-value < 0.05, fold change > 1.5, and > 10 transcripts per million (TPM) in at least one condition. T-bet-activated (orange), -repressed (blue), and -bound (+) genes (detected by T-bet ChIP-seq) are depicted. See also Table S1.

(B) Tracks of T-bet-activated and -repressed genes (*Ifng* and *Isg15*, respectively) show expression, enhancer marks (H3K4me1 and H3K27Ac), and T-bet binding. For each mark, WT and *Tbx21*^{-/-} cells are compared.

(C) GO analysis of the T-bet-activated and -repressed genes defined in Figure 1A. The top five pathways are listed for activated (orange) and repressed (blue) genes, including the enrichment p value, number of genes per pathway, and names of representative genes.

RESULTS

T-bet Represses Type I IFN Signature Genes in IFN- γ -Exposed CD4⁺ T Cells

To gain insight into the global change in transcription due to T-bet in CD4⁺ T cells, we first performed RNA sequencing (RNA-seq) to compare wild-type and *Tbx21*^{-/-} CD4⁺ T cells treated with IFN- γ (72 hr). Under the conditions used, the absence of T-bet altered the expression of 529 genes, roughly half of which (253) were induced and half of which (276) were repressed by T-bet (Figure 1A and Table S1). In contrast, *Tbx21* deletion had a minimal impact on IFN- β response (Figure S1). For genes affected by *Tbx21* deletion in the IFN- γ condition, T-bet chromatin immunoprecipitation sequencing (ChIP-seq) revealed that T-bet bound to 42% of T-bet-activated genes and 35% of T-bet-repressed genes. Tracks of representative genes regulated and bound by T-bet include *Ifng* (activated) and *Isg15* (repressed) (Figure 1B). Aside from *Isg15*, we noted other canonical type-I-IFN-induced genes in the T-bet-

repressed gene group, and Gene Ontology (GO) analysis of T-bet-repressed genes showed a highly significant enrichment for a type I IFN (IFN- β) response and anti-viral responses (Figure 1C). In contrast, the GO analysis of T-bet-activated genes showed enrichment of metabolic genes, including those encoding glycolytic enzymes (Figure 1C). This unexpected enrichment of a type I IFN signature in IFN- γ -treated T-bet-deficient CD4⁺ T cells points to a role for T-bet in repressing this transcriptomic program.

Distinctive Transcriptome Induced by IFN- γ Approximates IFN- β -Induced Transcriptome in the Absence of T-bet

This observation prompted us to directly compare the effects of IFN- β - and IFN- γ -regulated transcriptomes over time (6, 24, and 72 hr; Figure S2A). In T cells, IFN- β and IFN- γ had very different transcriptomic consequences and remarkably few commonly regulated genes (Figure S2B and Table S2). Moreover, IFN- β rapidly induced its canonical ISGs, whereas the main impact of

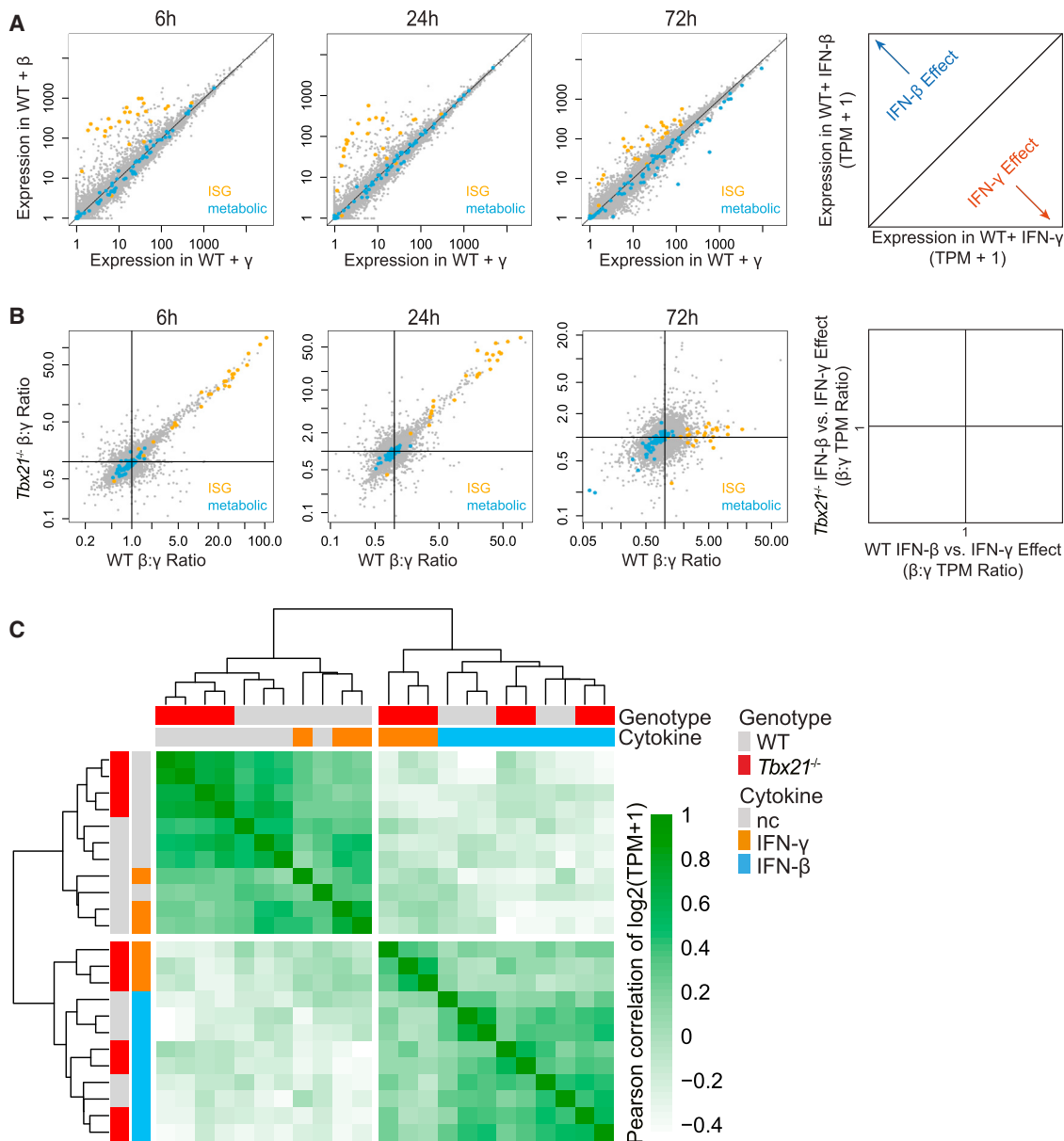


Figure 2. The Distinctive Transcriptome Induced by IFN- γ in the Absence of T-bet Approximates an IFN- β -Induced Transcriptome

(A) Scatterplots of gene expression induced by IFN- β versus IFN- γ in WT cells at 6 hr (IFN- β [n = 2] and IFN- γ [n = 2]), 24 hr (IFN- β [n = 2] and IFN- γ [n = 2]), and 72 hr (IFN- β [n = 5] and IFN- γ [n = 3]). See also [Figure S2A](#) and [Table S2](#). Canonical ISGs are marked in yellow, and metabolic genes are denoted in blue; all other genes are marked in gray.

(B) Scatterplots showing the effect of T-bet on differential IFN response. To depict differential expression between IFN- β and IFN- γ , fold changes (IFN- β /IFN- γ) in WT cells (x axis) and $Tbx21^{-/-}$ cells (y axis) are compared.

(C) Correlation heatmap of transcriptomes induced by IFN- β or IFN- γ of WT and $Tbx21^{-/-}$ cells at 72 hr of IFN exposure. The number of repeats for each condition is as follows: WT (no cytokine [n = 4], IFN- β [n = 5], and IFN- γ [n = 3]) and $Tbx21^{-/-}$ (no cytokine [n = 4], IFN- β [n = 4], and IFN- γ [n = 3]).

IFN- γ , as judged by GO analysis, was on metabolic genes that were modestly induced by this cytokine ([Figure 2A](#)). We next compared the effect of T-bet on differentiating IFN- γ and IFN- β effects (depicted as the ratio of expression levels, in transcripts per million [TPM], in IFN- β :IFN- γ conditions) by focusing on ISGs (highlighted in yellow; [Figure 2B](#)). Preferential ISG induction by IFN- β at early time points (6 and 24 hr) was largely independent of T-bet (the x axis value [wild-type] approximates the

y axis value [$Tbx21^{-/-}$]). However, at 72 hr, the preferential induction of ISGs by IFN- β was all but lost in $Tbx21^{-/-}$ cells, suggesting that the maintenance of differential responses to IFN- β and IFN- γ signals over time is T-bet dependent. Unbiased clustering of transcriptomic data at 72 hr placed all IFN- γ -treated $Tbx21^{-/-}$ samples with IFN- β treated samples, and they were clearly separable from wild-type IFN- γ samples. This suggests that the distinctiveness of the IFN- γ signal is not maintained in

the absence of T-bet and instead approximates an IFN- β signal (Figure 2C).

Aberrant STAT2 Activation in IFN- γ -Activated T-bet-Deficient Cells

To identify potential molecular mechanisms underlying the aberrant IFN response observed in *Tbx21*^{-/-} T cells, we considered whether T-bet alters intracellular IFN signaling. Type I IFNs activate a heterotrimeric complex comprising STAT1, STAT2, and IRF9 (originally called ISGF3), which bind to IFN-stimulated response element (ISRE) (Darnell et al., 1994; Stark et al., 1998). As shown in Figure 3A, IFN- β , but not IFN- γ , induced phosphorylation of STAT2 and augmented the level of total STAT2 in wild-type cells. However, in *Tbx21*^{-/-} T cells, both IFN- γ and IFN- β induced STAT2 phosphorylation and protein expression. Accordingly, the number of global STAT2 binding peaks detected by ChIP-seq was also higher in *Tbx21*^{-/-} cells than in wild-type cells (Figure 3B). Furthermore, localized accumulation of STAT2 binding around ISGs was also enhanced in *Tbx21*^{-/-} cells by IFN- γ and IFN- β (Figure 3C, upper panels) and was associated with enhanced active enhancer (H3K27Ac) marks (Figure 3C, lower panels). These results indicate that in *Tbx21*^{-/-} cells, IFN- γ aberrantly activates STAT2 and its binding to canonical ISGs with activation of nearby enhancers. We next investigated whether T-bet might directly interfere with STAT2 binding by comparing the overlap between T-bet and STAT2 binding sites. We found that up to 24% of T-bet binding sites overlapped STAT2, suggesting that direct competition is possible (Figure S3A).

T-bet-Repressed Genes Are Preferential Targets of STAT2, IRF7, and STAT1 in the Absence of T-bet

IRF7 is induced by and regulates type I IFN (Decker et al., 2005). We found that IRF7 levels were also aberrantly increased in response to IFN- γ in *Tbx21*^{-/-} cells (Figure S3B). We next considered the possibility that, in the absence of T-bet, key positive amplifiers for type I IFN signaling, such as STAT2, IRF7, and STAT1 (Mostafavi et al., 2016), might be enhanced and preferentially bound in proximity to genes normally repressed by T-bet (identified in Figure 1A and Table S1). We observed that, whereas binding of T-bet was more frequently evident near T-bet-activated genes than near T-bet-repressed genes, binding of STAT2, IRF7, and STAT1 occurred more frequently around genes normally repressed by T-bet (Figure 3D). The preferential targeting of T-bet-repressed genes by type I IFN TFs was intriguing and led us to expand our analysis to include multiple TF binding data in various conditions (summary data list in Table S3). Our multi-sample analysis revealed that preferential targeting of T-bet-repressed genes over T-bet-activated genes was a feature confined to specific factors (STAT2, STAT1, and IRF7) in specific conditions (the top four conditions in Figure 3E). It is of note that statistically significant preferential binding of STAT1 to T-bet-repressed genes was observed only in the context of IFN- γ -treated *Tbx21*^{-/-} cells but not in IFN- γ -treated wild-type cells, suggesting a global shift in STAT1 distribution in the absence of T-bet (Figure 3E, two rows colored in red). Representative examples of genes that are bound and repressed by T-bet and are also bound by STAT1, STAT2, and IRF7 are depicted in Figure S3C. Thus, our results suggest that

in the absence of T-bet, the genes normally repressed by T-bet become preferential targets of STAT2, IRF7, and STAT1 in response to IFN- γ .

Blocking Autocrine Type I IFNs Restores the Normal IFN- γ Transcriptomic Response in T-bet-Deficient T Cells

Type I IFN signaling circuitry consists of a self-reinforcing loop that incorporates autocrine production of IFN (Honda et al., 2006). Therefore, we anticipated that enhancement of three TFs that promote type I IFN responses could also lead to augmented type I IFN production. Indeed, we detected aberrantly high levels of IFN- α and IFN- β 1 transcripts in IFN- γ -treated T-bet-deficient cells (Figure S4A). This self-amplifying loop and production of autocrine type I IFNs was further suggested by the late appearance of a type I IFN signature in IFN- γ -treated *Tbx21*^{-/-} cells at 72 hr (Figure 2). To confirm this possibility, we added anti-IFN- α /beta receptor (IFNAR) antibody together with IFN- γ to *Tbx21*^{-/-} cells. We found that in a dose-dependent manner, anti-IFNAR antibody treatment restored a normal IFN- γ transcriptome (Figure 4A), attenuated the aberrantly enhanced ISG expression (Figure 4B and Figure S4B), and corrected the IFN- γ -triggered STAT2 activation (Figures 4C and 4D) in T-bet-deficient cells. Anti-IFNAR antibody also corrected the aberrant expression of type I IFN and IRF7 transcripts but had no effect on IRF3 (Figures S4A and S4C). Thus, the data reveal a previously unrecognized function of T-bet to constrain auto-amplifying type I IFN circuitry in an IFN- γ -abundant environment. In the absence of T-bet, T cells misperceive IFN- γ and are directed into a very different transcription program that approximates type I IFNs. It is of note, however, that some T-bet-mediated repression of ISGs could be direct, because 26% of ISGs are directly bound by T-bet (Figure 4B, black-and-white column on the left).

T-bet Selectively Constrains Type I IFN TFs and Represses Type I IFN Circuitry In Vivo

This action of T-bet as a repressor of type I IFN circuitry downstream of IFN- γ was unanticipated, so we sought to determine whether our in-vitro-based observations were relevant in vivo. We challenged mice with *Toxoplasma gondii*, a parasitic infection known to be a major inducer of IFN- γ (Gazzinelli et al., 1993). Because T-bet-deficient mice do not survive *T. gondii* infection as a result of the failure to systemically mount a protective Th1 response (Harms Pritchard et al., 2015), it was necessary to reconstitute *Rag2*^{-/-} mice with both wild-type and *Tbx21*^{-/-} naive T cells before infection. Consequently, these mice survived *T. gondii* infection upon challenge, and importantly, both populations of T cells experienced the same inflammatory environment before transcriptome analysis (Figure 5A). As a control, we also analyzed T cells from wild-type and *Tbx21*^{-/-} mice infected with lymphocytic choriomeningitis virus (LCMV), a viral infection known to induce a dynamic type I IFN response (Teijaro et al., 2013; Wilson et al., 2013; Zhou et al., 2010). As expected, unbiased hierarchical clustering of transcriptomes revealed that pathogen type (*T. gondii* or LCMV) and tissue location (splenocytes or peritoneal exudate cells [PECs]) were major determinants in distinguishing transcriptome profiles. Within these major clusters, cellular genotype (wild-type

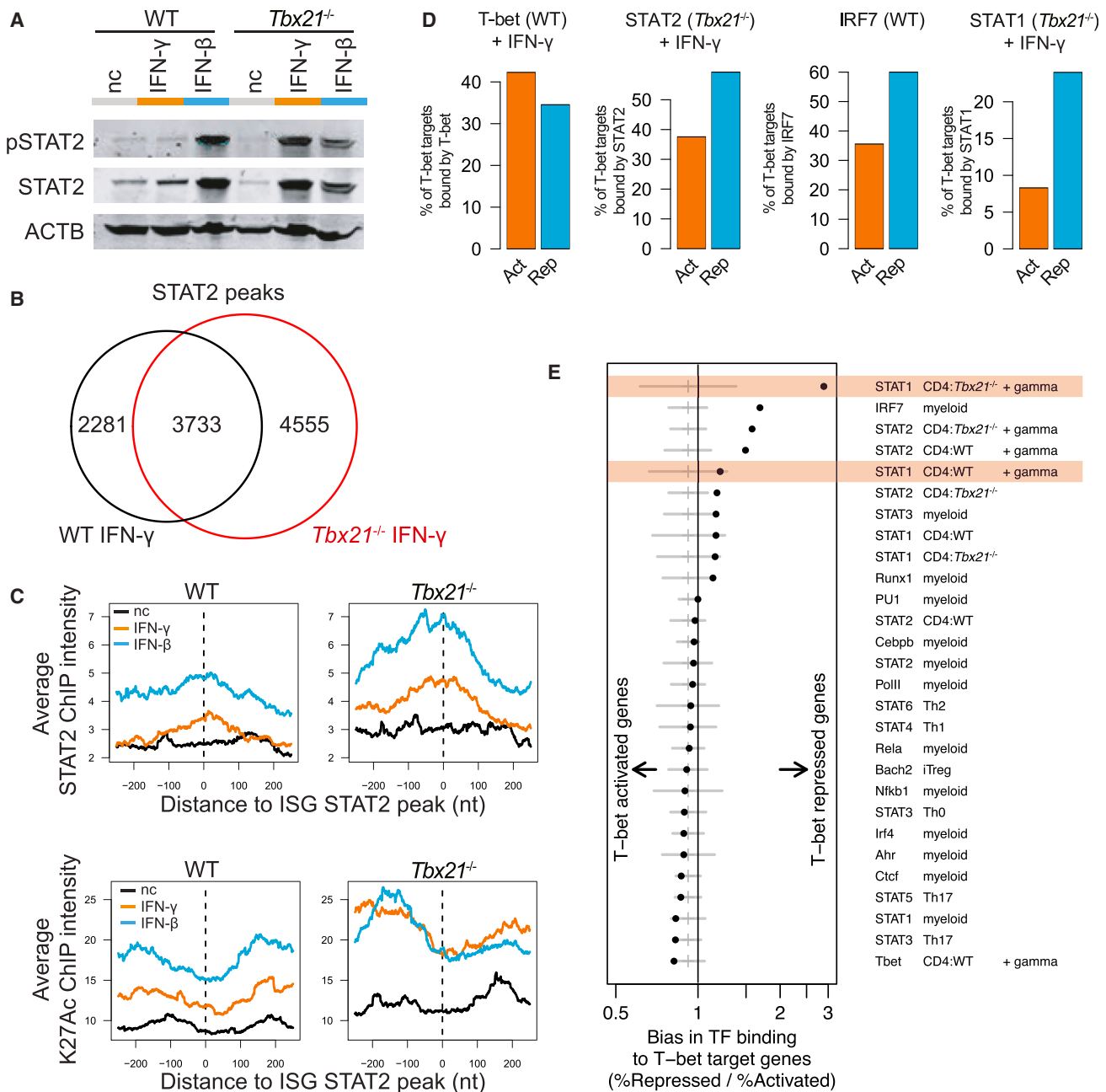


Figure 3. Aberrant STAT2 Activation in IFN- γ -Activated T-bet-Deficient Cells

(A) Western blot analysis of phospho-STAT2, total STAT2, and β -actin compares WT and *Tbx21*^{-/-} cells. For each genotype, three conditions (no cytokine, IFN- β , and IFN- γ) were tested.

(B) Overlapping and unique STAT2 binding peaks between WT and *Tbx21*^{-/-} cells treated with IFN- γ .

(C) Average STAT2 ChIP binding intensity (top panels) and H3K27Ac intensity (bottom panels) centered at STAT2 peaks of ISGs (27 genes). For WT (left panels) and *Tbx21*^{-/-} (right panels), three conditions are compared (no cytokines, IFN- γ , and IFN- β).

(D) TF binding to T-bet-activated and -repressed genes (as defined in Figure 1A). Genes exhibiting TF binding within 50 kb of the transcription start or end site or inside their gene bodies are counted as direct targets, and the percentage of direct targets was calculated for T-bet-activated and -repressed genes. TFs shown include T-bet, STAT1, and STAT2 in IFN- γ -treated T cells and IRF7 in macrophages (Cohen et al., 2014). See also Figure S3A.

(E) Distribution of TF binding to T-bet-activated versus T-bet-repressed genes. The analysis in (D) was expanded to include multiple TFs and conditions, some of which are available from public databases (Garber et al., 2012; Hirahara et al., 2015; Roychoudhuri et al., 2013; Vahedi et al., 2012; Wei et al., 2010; Yang et al., 2011; dataset sources are listed in Table S3). Gray bars represent the 95% confidence intervals and median biases expected by chance (see Star Methods for details). The biases observed in the top four rows were outside the median biases expected by chance and were therefore considered statistically significant (empirical p values < 1E-4). Two lanes of IFN- γ -induced STAT1 binding are highlighted for comparison, showing differential distribution in the presence (WT) or absence (*Tbx21*^{-/-}) of T-bet.

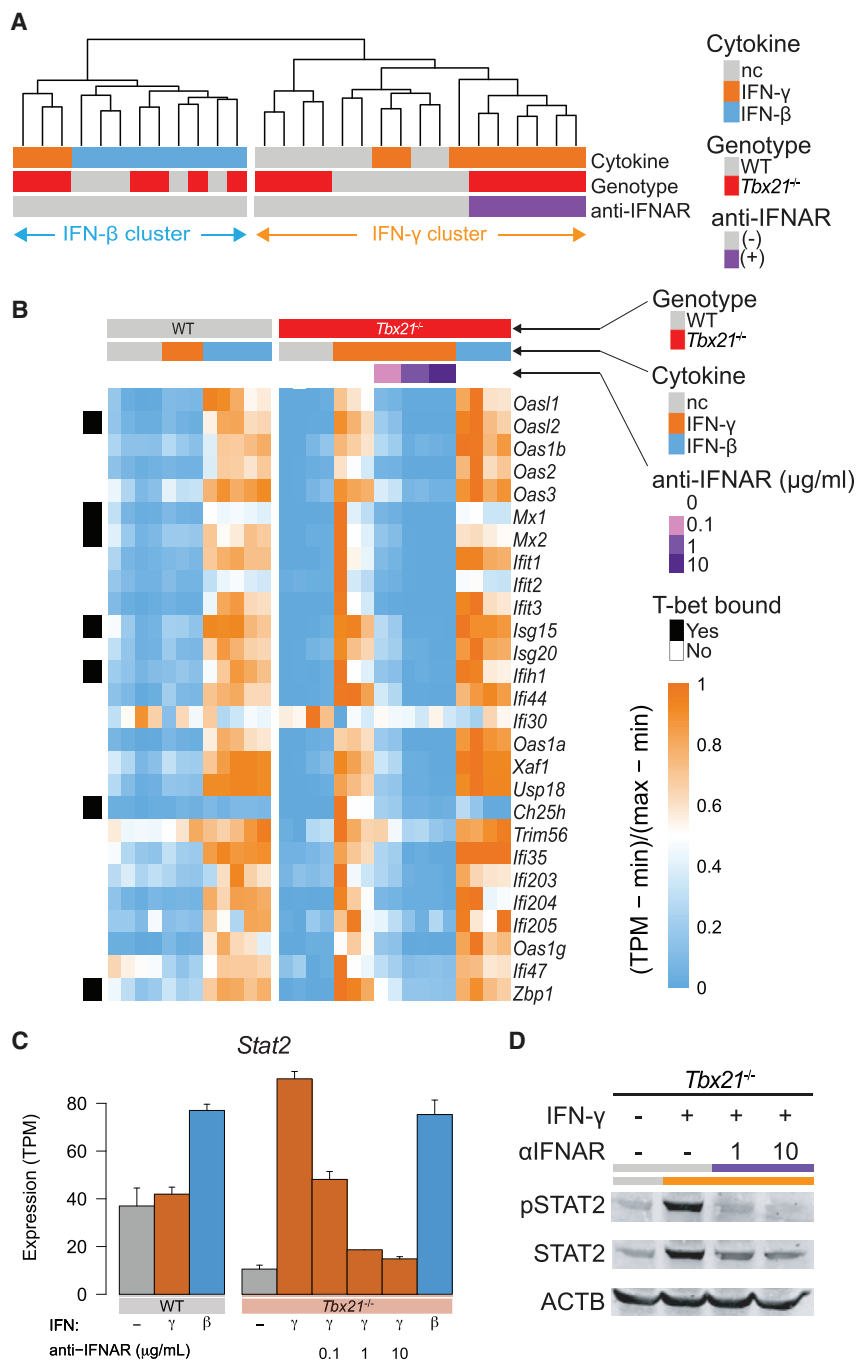


Figure 4. Blocking Autocrine Type I IFNs Restores Normal IFN- γ Transcriptomic Response in T-bet-Deficient T Cells

(A) Unbiased hierarchical clustering of 29 transcriptomes derived from WT and *Tbx21*^{-/-} cells cultured with or without IFN- γ or IFN- β and with or without anti-IFNAR antibody. The resultant dendrogram is shown, and samples are color coded in the legend for (1) the type of cytokine treatment (gray, no cytokine [nc]; orange, IFN- γ ; and blue, IFN- β), (2) cell genotype (gray, WT; and red, *Tbx21*^{-/-}), and (3) anti-IFNAR antibody treatment (gray, no antibody; and purple, antibody). The number of repeats included in each condition is as follows: WT (no cytokine [n = 4], IFN- β [n = 5], and IFN- γ [n = 3]) and *Tbx21*^{-/-} (no cytokine [n = 4], IFN- β [n = 4], IFN- γ [n = 3], and IFN- γ + anti-IFNAR [n = 6]).

(B) Heatmap showing relative gene expression of ISGs compares WT and *Tbx21*^{-/-} cells. The numbers of repeats included in each condition and the color coding of samples are the same as in (A). For anti-IFNAR treatment, three different doses were tested, and samples were acquired in duplicates per dose. The presence or absence of T-bet binding on each gene is shown on the left. See also Figure S4.

(C) Absolute gene expression (TPM) of STAT2 in nine different conditions. Data are expressed as mean TPM \pm SEM of n = 2–5.

(D) Western blot analysis of pSTAT2 and total STAT2 in IFN- γ -treated *Tbx21*^{-/-} cells with or without anti-IFNAR antibody.

ment during the infection, the results indicate that the observed hyperactivity of type I IFN circuitry in *Tbx21*^{-/-} cells is cell intrinsic during infection in vivo. In contrast, LCMV infection, which induces a dominant type I IFN response, showed no major impact of T-bet loss on selective expression of STATs or IRFs. Collectively these data indicate that T-bet is a blanket repressor of intrinsic type I IFN circuitry during a robust Th1 response.

DISCUSSION

The T-box family member T-bet was discovered in 2000 (Szabo et al., 2000) and identified to be a positive regulator

of IFN- γ , the signature cytokine of Th1 cells. In this study, we employed genomic approaches to unearth other important functions of T-bet not previously appreciated. Our work has revealed an intriguing action of T-bet as a LDTF that protects Th1 cells from amplifying aberrant type I IFN circuitry in an IFN- γ -abundant microenvironment. In this respect, our finding provides a very different view of a LDTF: not only does T-bet regulate IFN- γ production, but it also aids in interpreting the microenvironment it creates. The work also emphasizes that T-bet, in addition to playing a positive role in Th1 cell differentiation, has

or *Tbx21*^{-/-} or virus subtype (clone 13 [CI13] or Armstrong) contributed to separate subfractions (Figure 5B). Using this dataset, we sought to determine how positive amplifiers of IFN signaling, such as STATs and IRFs, were operating in vivo (Figure 5C). Interestingly, in *T. gondii*-infected PECs, the distinctive upregulation of type I IFN factors (STAT1, STAT2, IRF7, and IRF9) was evident in *Tbx21*^{-/-} cells (in comparison with wild-type cells), indicative of the amplified type I IFN circuitry that we first identified in vitro. Because wild-type and *Tbx21*^{-/-} T cells experienced the same inflammatory environ-

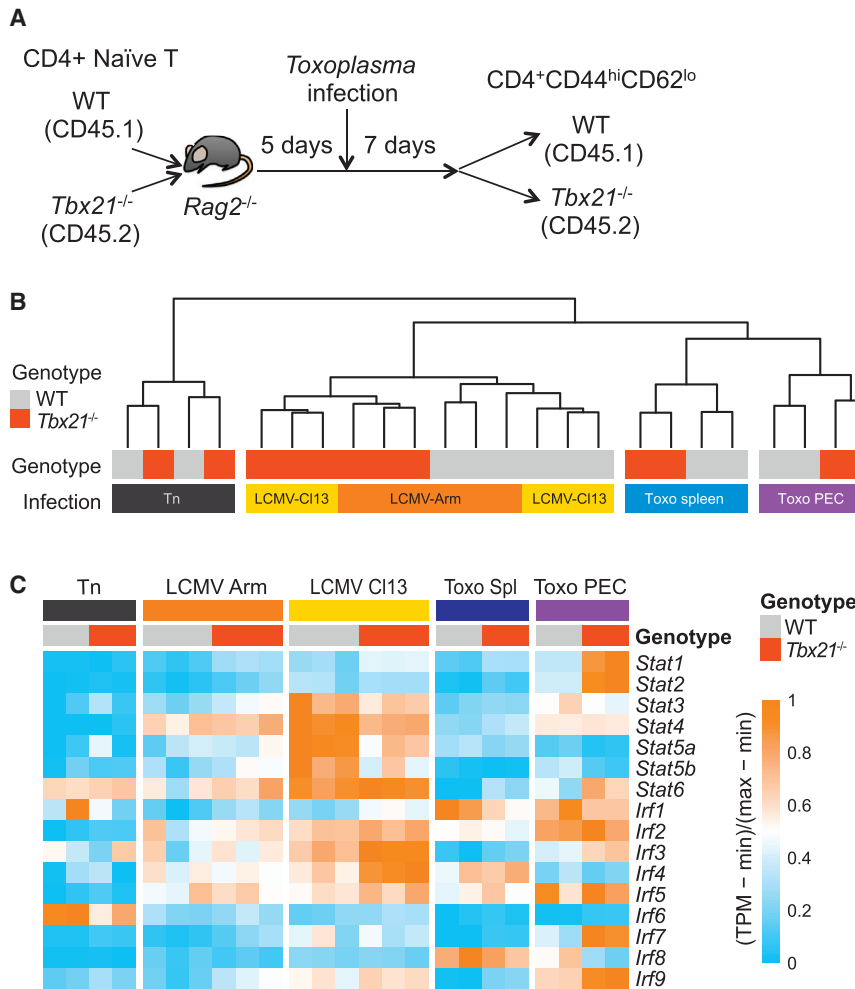


Figure 5. T-bet Selectively Constrains Type I IFN TFs and Represses Type I IFN Circuitry In Vivo

(A) Experimental design of *T. gondii* infection study.

(B) Unbiased clustering of transcriptomic data derived from 24 samples, including native uninfected cells (Tn) and infected cells (all others). Each sample is color coded for (1) cell genotype (gray, WT; and red, *Tbx21*^{-/-}) and (2) the type of infection and tissue location (black, uninfected naive T cells; brown, splenic T cells infected with LCMV Armstrong [LCMV-Arm]; yellow, splenic T cells infected with LCMV clone 13 [LCMV-CI13]; blue, *T. gondii*-infected splenic T cells; and purple, *T. gondii*-infected PECs). The number of repeats included in each condition is the same for both WT and *Tbx21*^{-/-} cells: (naive [n = 2], LCMV-CI13 [n = 3], LCMV-Arm [n = 3], *T. gondii* spleen [n = 2], and *T. gondii* PECs [n = 2]).

(C) Heatmap showing relative gene expression of STAT and IRF family TFs. Each sample is color coded for (1) the type of infection and tissue location (black, uninfected naive T cells; brown, splenic T cells infected with LCMV-Arm; yellow, splenic T cells infected with LCMV-CI13; blue, *T. gondii*-infected splenic T cells; and purple, *T. gondii*-infected PECs) and (2) cell genotype (gray, WT; and red, *Tbx21*^{-/-}).

complex to construct a feed-forward circuit. A consequence of this amplification loop is the induction of the components of both phases, such that IRF and STAT family members are themselves induced by IFNs. IFN- γ is a specialized factor that acts through a distinct receptor and SDTF, a STAT1

essential functions in repressing and influencing multiple key components of a collateral type I IFN signaling circuitry.

Our investigation into the actions of T-bet revealed a multifaceted mechanism by which T-bet constrains type I IFN production and signaling. In the absence of T-bet, we observed (1) selective, cell-intrinsic upregulation of type I IFN TFs (STAT1, STAT2, IRF7, and IRF9) among all STAT and IRF families; (2) preferential binding of STAT1, STAT2, and IRF7 to normally T-bet-repressed genes; (3) enhanced expression of type I IFNs and ISG transcripts; (4) direct T-bet binding near 26% of ISGs; and (5) effective cancellation of aberrant ISG induction by the blocking of IFN receptor signaling. Collectively, our findings suggest that two molecular mechanisms of T-bet most likely coexist: (1) repression of type I IFN production and downstream activity of signaling molecules STAT1, STAT2, IRF7, and IRF9; and (2) direct binding and repression of ISGs.

Multiple factors contribute to the sensing of foreign nucleic acids and bacterial products, which in turn lead to the production of a large family of related cytokines, the type I IFNs (Honda et al., 2006). This initial production of type I IFNs is amplified by a secondary phase in which IFNs act in an autocrine and paracrine manner via IFNAR and the STAT1-STAT2-IRF9 multiprotein

homodimer (Darnell et al., 1994). Strikingly, our work shows that IFN- γ mimics the actions of type I IFNs unless T-bet is present. Our evidence showing that anti-IFNAR effectively abrogates the aberrant type I IFN signature in T-bet-deficient cells points to the importance of T-bet in preventing the type I IFN amplification phase. Although we cannot discern the very first molecular event that triggers the production of type I IFNs downstream of IFN- γ , we can postulate that a transient, low-level triggering of type I IFN signaling could underlie the recently described tonic IFN phenotype (Mostafavi et al., 2016). To keep type I IFN signaling in check, multiple negative-feedback mechanisms, including recent findings on STAT2 and USP18 (Arimoto et al., 2017) or ISG15 (Zhang et al., 2015), are in place. Here, we add T-bet as a context-dependent negative regulator that has non-redundant, critical functions operative in IFN- γ -producing Th1 cells.

It is also of note that the context in which T-bet acts to restrain type I IFN signaling appears to be relatively specific to IFN- γ -rich conditions and not IFN- β -abundant settings. This context dependence is probably one reason why T-bet deletion had a greater impact on gene expression in the *T. gondii* infection model (which is a dominant IFN- γ response) than in the LCMV infection model (which produces a dominant type I IFN

response). Our T cell co-transfer experiment of wild-type and T-bet-deficient T cells for *T. gondii* infection also points to the T-cell-intrinsic nature of auto-amplification of type I IFN signaling in the absence of T-bet. It is tempting to speculate that this constraint of the type I IFN signature is an important factor in maintaining the fitness of CD4 T cells during a vigorous Th1-cell-inducing infection. Our work also raises a possibility of disease relevance in which the aberrant type I IFN signature associated with various autoimmune conditions could be the result of an IFN- γ -dominant environment in which there is impairment in T-bet expression or function.

It is generally appreciated that LDTFs such as T-bet promote specification of their cognate lineage and restrict alternative fates. For instance, LDTFs can limit the production of factors that drive the generation of alternate lineages (Zhu et al., 2010). The present data provide a different, interesting wrinkle on this theme whereby an LDTF influences how the cell “sees” its secreted product; evidently, T cells sense type I and type II IFNs as similar stimuli unless T-bet is present. It will be of fundamental interest to discern how many LDTFs have this capacity. In addition, many LDTFs are referred to as transcriptional activators or repressors, but our work on T-bet provides a striking example of how nuanced this classification can be. Our ChIP-seq data indicate that T-bet is an activator about half of the time and acts as a repressor the other half. This observation prompts the question as to how T-bet knows how it should act on any given locus. Presumably, the action of T-bet is greatly influenced by its collaborative molecular partners (Djuretic et al., 2007; Dominguez et al., 2015) and the chromatin conformation or looping (Liu et al., 2016; Sekimata et al., 2009). However, this raises another question: how does T-bet know where and whom to partner with? Logically, one would assume that this information is encoded in the genome, but defining how DNA sequence gives rise to the locus-specific combinatorial logic will be of great interest for future exploration.

STAR★METHODS

Detailed methods are provided in the online version of this paper and include the following:

- KEY RESOURCES TABLE
- CONTACT FOR REAGENT AND RESOURCE SHARING
- EXPERIMENTAL MODEL AND SUBJECT DETAILS
- METHOD DETAILS
 - Mice and Media
 - Cell Culture
 - Flow Cytometry
 - Immunoblot Analysis
 - RNA Sequencing
 - ChIP-Seq
 - *T. gondii* Infection
 - LCMV Infection
- QUANTIFICATION AND STATISTICAL ANALYSIS
 - RNA-Seq Analysis
 - Evaluating Functional Enrichment
 - ChIP-Seq Analysis
- DATA AND SOFTWARE AVAILABILITY

SUPPLEMENTAL INFORMATION

Supplemental Information include four figures and three tables and can be found with this article online at <http://dx.doi.org/10.1016/j.immuni.2017.05.005>.

AUTHOR CONTRIBUTIONS

Conceptualization, S.I. and J.J.O.; Methodology, S.I. and Y.M.; Software, F.P.D., H.-W.S., S.R.B., A.O., and H.-Y.S.; Validation, S.I., Y.M., and F.P.D.; Formal Analysis, F.P.D.; Investigation, S.I., Y.M., D.J., K.H., T.K., K.J., and Y.K.; Writing, Y.K. and J.J.O.; Visualization, F.P.D. and Y.M.; Supervision, T.N., A.S., and J.J.O.; Funding Acquisition, A.S. and J.J.O.

ACKNOWLEDGMENTS

We thank J. Simone, J. Lay, and K. Tinsley from NIAMS and T. Moyer from NIAID for expert assistance in flow cytometry and the NIAMS LACU staff for their excellent technical support in handling mice. We thank G. Gutierrez-Cruz for deep-sequencing support. This study utilized the high-performance computational capabilities of the Biowulf Linux cluster at the NIH. This work was supported by the Intramural Research Programs of NIAMS and NIAID.

Received: January 11, 2017

Revised: March 10, 2017

Accepted: March 31, 2017

Published: June 13, 2017

REFERENCES

- Arimoto, K.-I., Löchte, S., Stoner, S.A., Burkart, C., Zhang, Y., Miyauchi, S., Wilmes, S., Fan, J.-B., Heinisch, J.J., Li, Z., et al. (2017). STAT2 is an essential adaptor in USP18-mediated suppression of type I interferon signaling. *Nat. Struct. Mol. Biol.* 24, 279–289.
- Boehm, U., Klamp, T., Groot, M., and Howard, J.C. (1997). Cellular responses to interferon-gamma. *Annu. Rev. Immunol.* 15, 749–795.
- Bray, N.L., Pimentel, H., Melsted, P., and Pachter, L. (2016). Near-optimal probabilistic RNA-seq quantification. *Nat. Biotechnol.* 34, 525–527.
- Cohen, M., Matcovitch, O., David, E., Barnett-Itzhaki, Z., Keren-Shaul, H., Blecher-Gonen, R., Jaitin, D.A., Sica, A., Amit, I., and Schwartz, M. (2014). Chronic exposure to TGF β 1 regulates myeloid cell inflammatory response in an IRF7-dependent manner. *EMBO J.* 33, 2906–2921.
- Darnell, J.E.J., Jr., Kerr, I.M., and Stark, G.R. (1994). Jak-STAT pathways and transcriptional activation in response to IFNs and other extracellular signaling proteins. *Science* 264, 1415–1421.
- Decker, T., Müller, M., and Stockinger, S. (2005). The yin and yang of type I interferon activity in bacterial infection. *Nat. Rev. Immunol.* 5, 675–687.
- Djuretic, I.M., Levanon, D., Negreanu, V., Groner, Y., Rao, A., and Ansel, K.M. (2007). Transcription factors T-bet and Runx3 cooperate to activate Ifng and silence Il4 in T helper type 1 cells. *Nat. Immunol.* 8, 145–153.
- Dobin, A., Davis, C.A., Schlesinger, F., Drenkow, J., Zaleski, C., Jha, S., Batut, P., Chaisson, M., and Gingeras, T.R. (2013). STAR: ultrafast universal RNA-seq aligner. *Bioinformatics* 29, 15–21.
- Dominguez, C.X., Amezquita, R.A., Guan, T., Marshall, H.D., Joshi, N.S., Kleinstein, S.H., and Kaech, S.M. (2015). The transcription factors ZEB2 and T-bet cooperate to program cytotoxic T cell terminal differentiation in response to LCMV viral infection. *J. Exp. Med.* 212, 2041–2056.
- Dunn, G.P., Koebel, C.M., and Schreiber, R.D. (2006). Interferons, immunity and cancer immunoediting. *Nat. Rev. Immunol.* 6, 836–848.
- Falcon, S., and Gentleman, R. (2007). Using GOstats to test gene lists for GO term association. *Bioinformatics* 23, 257–258.
- Garber, M., Yosef, N., Goren, A., Raychowdhury, R., Thielke, A., Guttman, M., Robinson, J., Minie, B., Chevrier, N., Itzhaki, Z., et al. (2012). A high-throughput chromatin immunoprecipitation approach reveals principles of dynamic gene regulation in mammals. *Mol. Cell* 47, 810–822.

- Gazzinelli, R.T., Denkers, E.Y., and Sher, A. (1993). Host resistance to *Toxoplasma gondii*: model for studying the selective induction of cell-mediated immunity by intracellular parasites. *Infect. Agents Dis.* 2, 139–149.
- Guo, Y., Mahony, S., and Gifford, D.K. (2012). High resolution genome wide binding event finding and motif discovery reveals transcription factor spatial binding constraints. *PLoS Comput. Biol.* 8, e1002638.
- Harms Pritchard, G., Hall, A.O., Christian, D.A., Wagage, S., Fang, Q., Muallem, G., John, B., Glatman Zaretsky, A., Dunn, W.G., Perrigoue, J., et al. (2015). Diverse roles for T-bet in the effector responses required for resistance to infection. *J. Immunol.* 194, 1131–1140.
- Heinz, S., Romanoski, C.E., Benner, C., and Glass, C.K. (2015). The selection and function of cell type-specific enhancers. *Nat. Rev. Mol. Cell Biol.* 16, 144–154.
- Hirahara, K., Onodera, A., Villarino, A.V., Bonelli, M., Sciumè, G., Laurence, A., Sun, H.-W., Brooks, S.R., Vahedi, G., Shih, H.-Y., et al. (2015). Asymmetric Action of STAT Transcription Factors Drives Transcriptional Outputs and Cytokine Specificity. *Immunity* 42, 877–889.
- Honda, K., Takaoka, A., and Taniguchi, T. (2006). Type I interferon gene induction by the interferon regulatory factor family of transcription factors. *Immunity* 25, 349–360.
- Jankovic, D., Kullberg, M.C., Feng, C.G., Goldszmid, R.S., Collazo, C.M., Wilson, M., Wynn, T.A., Kamanaka, M., Flavell, R.A., and Sher, A. (2007). Conventional T-bet(+)Foxp3(-) Th1 cells are the major source of host-protective regulatory IL-10 during intracellular protozoan infection. *J. Exp. Med.* 204, 273–283.
- Kent, W.J., Zweig, A.S., Barber, G., Hinrichs, A.S., and Karolchik, D. (2010). BigWig and BigBed: enabling browsing of large distributed datasets. *Bioinformatics* 26, 2204–2207.
- Langmead, B., Trapnell, C., Pop, M., and Salzberg, S.L. (2009). Ultrafast and memory-efficient alignment of short DNA sequences to the human genome. *Genome Biol.* 10, R25.
- Liu, C.F., Brandt, G.S., Hoang, Q.Q., Naumova, N., Lazarevic, V., Hwang, E.S., Dekker, J., Glimcher, L.H., Ringe, D., and Petsko, G.A. (2016). Crystal structure of the DNA binding domain of the transcription factor T-bet suggests simultaneous recognition of distant genome sites. *Proc. Natl. Acad. Sci. USA* 113, E6572–E6581.
- Mostafavi, S., Yoshida, H., Moodley, D., LeBoité, H., Rothamel, K., Raj, T., Ye, C.J., Chevrier, N., Zhang, S.-Y., Feng, T., et al.; Immunological Genome Project Consortium (2016). Parsing the Interferon Transcriptional Network and Its Disease Associations. *Cell* 164, 564–578.
- Pimentel, H.J., Bray, N., Puente, S., Melsted, P., and Pachter, L. (2016). Differential analysis of RNA-Seq incorporating quantification uncertainty. *bioRxiv*. <http://dx.doi.org/10.1101/058164>.
- Quinlan, A.R., and Hall, I.M. (2010). BEDTools: a flexible suite of utilities for comparing genomic features. *Bioinformatics* 26, 841–842.
- Roychoudhuri, R., Hirahara, K., Mousavi, K., Clever, D., Klebanoff, C.A., Bonelli, M., Sciumè, G., Zare, H., Vahedi, G., Dema, B., et al. (2013). BACH2 represses effector programs to stabilize T(reg)-mediated immune homeostasis. *Nature* 498, 506–510.
- Sallusto, F. (2016). Heterogeneity of Human CD4(+) T Cells Against Microbes. *Annu. Rev. Immunol.* 34, 317–334.
- Schneider, W.M., Chevillotte, M.D., and Rice, C.M. (2014). Interferon-stimulated genes: a complex web of host defenses. *Annu. Rev. Immunol.* 32, 513–545.
- Sekimata, M., Pérez-Melgosa, M., Miller, S.A., Weinmann, A.S., Sabo, P.J., Sandstrom, R., Dorschner, M.O., Stamatiyannopoulos, J.A., and Wilson, C.B. (2009). CCCTC-binding factor and the transcription factor T-bet orchestrate T helper 1 cell-specific structure and function at the interferon-gamma locus. *Immunity* 31, 551–564.
- Stark, G.R., Kerr, I.M., Williams, B.R., Silverman, R.H., and Schreiber, R.D. (1998). How cells respond to interferons. *Annu. Rev. Biochem.* 67, 227–264.
- Suzuki, R., Leach, S., Liu, W., Ralston, E., Scheffel, J., Zhang, W., Lowell, C.A., and Rivera, J. (2014). Molecular editing of cellular responses by the high-affinity receptor for IgE. *Science* 343, 1021–1025.
- Szabo, S.J., Kim, S.T., Costa, G.L., Zhang, X., Fathman, C.G., and Glimcher, L.H. (2000). A novel transcription factor, T-bet, directs Th1 lineage commitment. *Cell* 100, 655–669.
- Teijaro, J.R., Ng, C., Lee, A.M., Sullivan, B.M., Sheehan, K.C.F., Welch, M., Schreiber, R.D., de la Torre, J.C., and Oldstone, M.B. (2013). Persistent LCMV infection is controlled by blockade of type I interferon signaling. *Science* 340, 207–211.
- Theofilopoulos, A.N., Baccala, R., Beutler, B., and Kono, D.H. (2005). Type I interferons (α/β) in immunity and autoimmunity. *Annu. Rev. Immunol.* 23, 307–336.
- Thorvaldsdóttir, H., Robinson, J.T., and Mesirov, J.P. (2013). Integrative Genomics Viewer (IGV): high-performance genomics data visualization and exploration. *Brief. Bioinform.* 14, 178–192.
- Vahedi, G., Takahashi, H., Nakayama, S., Sun, H.-W., Sartorelli, V., Kanno, Y., and O’Shea, J.J. (2012). STATs shape the active enhancer landscape of T cell populations. *Cell* 151, 981–993.
- Wei, L., Vahedi, G., Sun, H.-W., Watford, W.T., Takatori, H., Ramos, H.L., Takahashi, H., Liang, J., Gutierrez-Cruz, G., Zang, C., et al. (2010). Discrete roles of STAT4 and STAT6 transcription factors in tuning epigenetic modifications and transcription during T helper cell differentiation. *Immunity* 32, 840–851.
- Wilson, E.B., Yamada, D.H., Elsaesser, H., Herskovitz, J., Deng, J., Cheng, G., Aronow, B.J., Karp, C.L., and Brooks, D.G. (2013). Blockade of chronic type I interferon signaling to control persistent LCMV infection. *Science* 340, 202–207.
- Yang, X.-P., Ghoreschi, K., Steward-Tharp, S.M., Rodriguez-Canales, J., Zhu, J., Grainger, J.R., Hirahara, K., Sun, H.-W., Wei, L., Vahedi, G., et al. (2011). Opposing regulation of the locus encoding IL-17 through direct, reciprocal actions of STAT3 and STAT5. *Nat. Immunol.* 12, 247–254.
- Yates, A., Akanni, W., Amode, M.R., Barrell, D., Billis, K., Carvalho-Silva, D., Cummins, C., Clapham, P., Fitzgerald, S., Gil, L., et al. (2016). Ensembl 2016. *Nucleic Acids Res.* 44 (D1), D710–D716.
- Yosef, N., and Regev, A. (2016). Writ large: Genomic dissection of the effect of cellular environment on immune response. *Science* 354, 64–68.
- Zhang, Y., Liu, T., Meyer, C.A., Eeckhoutte, J., Johnson, D.S., Bernstein, B.E., Nussbaum, C., Myers, R.M., Brown, M., Li, W., and Liu, X.S. (2008). Model-based analysis of ChIP-Seq (MACS). *Genome Biol.* 9, R137.
- Zhang, X., Bogunovic, D., Payelle-Brogard, B., Francois-Newton, V., Speer, S.D., Yuan, C., Volpi, S., Li, Z., Sanal, O., Mansouri, D., et al. (2015). Human intracellular ISG15 prevents interferon- α/β over-amplification and auto-inflammation. *Nature* 517, 89–93.
- Zhou, S., Cerny, A.M., Zacharia, A., Fitzgerald, K.A., Kurt-Jones, E.A., and Finberg, R.W. (2010). Induction and inhibition of type I interferon responses by distinct components of lymphocytic choriomeningitis virus. *J. Virol.* 84, 9452–9462.
- Zhu, J., Yamane, H., and Paul, W.E. (2010). Differentiation of effector CD4 T cell populations (*). *Annu. Rev. Immunol.* 28, 445–489.

STAR★METHODS

KEY RESOURCES TABLE

REAGENT or RESOURCE	SOURCE	IDENTIFIER
Antibodies		
Anti-STAT1 antibody	Santa Cruz Biotechnology	sc-592; RRID: AB_632434
Anti-STAT2 antibody	Abcam	ab124283; RRID: AB_10971219
Anti-T-bet antibody	Santa Cruz Biotechnology	sc-21003; RRID: AB_2200557
Anti-H3K27Ac antibody	Abcam	ab4729; RRID: AB_2118291
Anti-H3K4m1 antibody	Abcam	ab8895; RRID: AB_306847
Anti-STAT2 antibody	EMD Millipore	07-140; RRID: AB_310391
Anti-STAT2 antibody (phospho-Tyr689)	LifeSpan Biosciences	LS-C10379-200; RRID: AB_866420
Anti-CD3 antibody	Thermo Fisher Scientific	16-0031-86; RRID: AB_468849
Anti-CD28 antibody	Thermo Fisher Scientific	16-0281-86; RRID: AB_468923
Anti-IFN- γ antibody	BioXCell	BE0055; RRID: AB_1107694
Anti-IL-4 antibody	BioXCell	BE0045; RRID: AB_1107707
Anti-CD4 antibody	BD Biosciences	550954; RRID: AB_393977
Anti-CD25 antibody	Thermo Fisher Scientific	17-0251-81; RRID: AB_469365
Anti-CD44 antibody	Thermo Fisher Scientific	11-0441-81; RRID: AB_465044
Anti-CD44 antibody	Thermo Fisher Scientific	12-0441-81; RRID: AB_465663
Anti-CD45.1 antibody	Thermo Fisher Scientific	17-0453-81; RRID: AB_465663
Anti-CD45.2 antibody	Thermo Fisher Scientific	48-0454-80; RRID: AB_11039533
Anti-CD62L antibody	Thermo Fisher Scientific	25-0621-81; RRID: AB_469632
Anti-CD62L antibody	Thermo Fisher Scientific	17-0621-81; RRID: AB_469409
Anti-Gr-1 antibody	Thermo Fisher Scientific	12-5931-81; RRID: AB_466044
Anti-NK1.1 antibody	Thermo Fisher Scientific	12-5941-63; RRID: AB_466048
Anti-IRF7 antibody	Thermo Fisher Scientific	12-5829-80; RRID: AB_2572628
Anti-IFNAR1 antibody	Thermo Fisher Scientific	16-5945-85; RRID: AB_1210688
Mouse IgG1 K isotype control	Thermo Fisher Scientific	14-4714-85; RRID: AB_470112
Bacterial and Virus Strains		
<i>Toxoplasma gondii</i>	Jankovic et al., 2007	N/A, generated in house
Lymphocytic Choriomeningitis Virus (Armstrong)	this paper	N/A, generated in house
Lymphocytic Choriomeningitis Virus (Clone 13)	this paper	N/A, generated in house
Chemicals, Peptides, and Recombinant Proteins		
Recombinant Mouse IFN- γ	R&D Systems	485-MI-100
Mouse IFN Beta	PBL interferon source	12400-1
Critical Commercial Assays		
TruSeq RNA Sample Prep Kit v2	Illumina	RS-122-2001
Deposited Data		
Raw and analyzed data	this paper	GEO: GSE96724
ENSEMBL release 82 GRCh38	Yates et al., 2016	http://www.ensembl.org/index.html
ChIP-seq samples for IRF7	Cohen et al., 2014	GEO: GSM1531571
Experimental Models: Organisms/Strains		
C57BL/6J	The Jackson Laboratory	000664
B6.SJL-PtprcaPep3b/BoyJ (CD45.1 ⁺)	The Jackson Laboratory	002014
C.B6 (Cg)-Rag2tm1.1Cgn/J (<i>Rag2</i> ^{-/-})	The Jackson Laboratory	008448
B6.129S6-Tbx21tm1Glm/J (<i>Tbx21</i> ^{-/-})	The Jackson Laboratory	004648

(Continued on next page)

Continued

REAGENT or RESOURCE	SOURCE	IDENTIFIER
Software and Algorithms		
STAR Aligner v2.4.2a	Dobin et al., 2013	https://github.com/alexdobin/STAR
BEDTOOLS v2.15	Quinlan and Hall, 2010	http://bedtools.readthedocs.io/en/latest/index.html
wigToBigWig	Kent et al., 2010	https://genome.ucsc.edu/goldenpath/help/bigWig.html
Integrative Genomics Viewer (IGV)	Thorvaldsdóttir et al., 2013	http://software.broadinstitute.org/software/igv/
kallisto v0.42.4	Bray et al., 2016	https://pachterlab.github.io/kallisto/
sleuth	Pimentel et al., 2016	http://pachterlab.github.io/sleuth/
pheatmap R package	Raivo Kolde	https://cran.r-project.org/web/packages/pheatmap/index.html
GOstats R package	Falcon and Gentleman, 2007	https://www.bioconductor.org/packages/release/bioc/html/GOstats.html
Bowtie v1.1.2	Langmead et al., 2009	http://bowtie-bio.sourceforge.net/index.shtml
MACS v1.4.3	Zhang et al., 2008	http://liulab.dfci.harvard.edu/MACS/index.html
GEM v2.6	Guo et al., 2012	http://groups.csail.mit.edu/cgs/gem/
BEDTOOLS v2.24	Quinlan and Hall, 2010	http://bedtools.readthedocs.io/en/latest/

CONTACT FOR REAGENT AND RESOURCE SHARING

Further information and requests for resources and reagents should be directed to and will be fulfilled by the Lead Contact, Yuka Kanno (kannoy@mail.nih.gov).

EXPERIMENTAL MODEL AND SUBJECT DETAILS

All animal experiments were performed in the AAALAC-accredited animal housing facilities at NIH. All animal studies were performed according to the NIH guidelines for the use and care of live animals and were approved by the Institutional Animal Care and Use Committee of NIAMS. Female mice of 8–12 weeks old were used in all experiments. For sample size, see corresponding figure legends.

METHOD DETAILS

Mice and Media

C57BL/6J, B6.SJL-PtprcaPep3b/BoyJ (CD45.1+), C.B6 (Cg)-*Rag2tm1.1Cgn/J* (*Rag2*^{-/-}), and B6.129S6-*Tbx21tm1Glm/J* (*Tbx21*^{-/-}) were purchased. All primary T cells isolated from mice were cultured in RPMI medium with 10% (vol/vol) FCS, 2 mM glutamine, 100 IU/mL of penicillin, 0.1 mg/mL of streptomycin and 20 mM HEPES buffer, pH 7.2–7.5 (all from Invitrogen), 1 mM sodium pyruvate, nonessential amino acids (gibco), and 2 μ M β -mercaptoethanol (Sigma-Aldrich).

Cell Culture

CD4⁺ T cells from spleens and lymph nodes of 6- to 8-week-old mice were purified by negative selection and magnetic separation (Miltenyi Biotec) followed by sorting of naive CD4⁺CD62L⁺CD44⁻CD25⁻ population using FACS Aria III or FACS Aria Fusion (BD). Naive CD4 T cells were activated by plate-bound anti-CD3 (10 μ g/mL, Clone: 145-2C11) and anti-CD28 (10 μ g/mL, 37.51) in media for 3 days either under neutral conditions or with IFN- γ (100 ng/mL, R&D Systems) or IFN- β (5000 U/mL, PBL interferon source).

Flow Cytometry

Flow cytometry analysis was performed on a FACSVerse, FACS Aria III or FACS Aria Fusion (BD). Acquired data were analyzed with FlowJo software (TreeStar).

For cell surface staining, the following anti-mouse antibodies were used: anti-CD4 (GK1.5), anti-CD25 (PC61.5), anti-CD44 (IM7), anti-CD45.1 (A20), anti-CD45.2 (104), anti-CD62L (MEL-14), anti-Gr-1 (RB6-8C5), and anti-NK-1.1 (PK136). For staining transcription factors, cells were fixed and permeabilized with Lyse/Fix Buffer and Perm Buffer III (BD), and were stained with anti-IRF7 (MNGPKL).

Immunoblot Analysis

Cultured cells were lysed as previously described (Suzuki et al., 2014). Cell lysates were fractionated by PAGE and transferred to a nitrocellulose membrane. After the membrane was blocked with Odyssey Blocking Buffer (LI-COR Biosciences), levels of STAT2 (EMD Millipore, 07-140), p-STAT2 (Lifespan Biosciences, LS-C10379), and actin (EMD Millipore, MAB1501R) were detected.

Secondary antibodies conjugated with IRDye800-conjugated (Rockland) and Alexa Fluor 680-conjugated (Invitrogen) were used for detection, and specific bands were visualized using Odyssey infrared imaging system (LI-COR Biosciences).

RNA Sequencing

RNA Sequencing (RNA-seq) was performed and analyzed as described previously. Total RNA was prepared from approximately 1 million cells by using TRIzol or mirVana miRNA Isolation Kit (Thermo Fisher Scientific). 200 ng of total RNA was subsequently used to prepare RNA-seq library by using TruSeq SR RNA sample prep kit (FC-122-1001, Illumina) by following manufacturer's protocol. The libraries were sequenced for 50 cycles (single read) with a HiSeq 2000 or HiSeq 2500 (Illumina). Raw sequencing data were processed with CASAVA 1.8.2 to generate FastQ files.

ChIP-Seq

Naive CD4 T cells were activated by plate-bound anti-CD3/CD28 (10 μ g/mL) for 3 days either under neutral conditions (anti-IL-4 [10 μ g/mL, 11B11] and anti-IFN- γ antibodies [10 μ g/mL, XMG1.2]) or with IFN- γ (100 ng/mL) and anti-IL-4 antibody. Cells cultured as indicated were cross-linked for 10 min with 1% formaldehyde and harvested. Cells were lysed by sonication and immunoprecipitated with anti-T-bet (sc-21003, Santa Cruz Biotechnology), anti-STAT1 (sc-592, Santa Cruz Biotechnology), anti-STAT2 (ab124283, AbCam), anti-H3K4m1 (ab8895, AbCam), and anti-H3K27ac (ab4729, AbCam). Recovered DNA fragments were blunt-end ligated to the Illumina adaptors, amplified, and sequenced for 50 cycles (single end) using the Hi-Seq 2000 or HiSeq 2500 (Illumina).

T. gondii Infection

We generated chimeric *Rag2*^{-/-} mice, reconstituted with ~5 million WT (CD45.1) and ~5 million *Tbx21*^{-/-} (CD45.2) naive CD4+ T cells sorted from Age- and Sex-matched mice (Figure 5A), and 5 days later i.p. infected them with approximately 20 cysts of the avirulent ME49 strain of *T. gondii* as described previously (Jankovic et al., 2007). Splenocytes and peritoneal exudate cells (PEC) were harvested at day 7 after the infection, and WT and *Tbx21*^{-/-} CD4+ CD62L^{lo} CD44^{hi} NK1.1- GR-1- T cells were sorted based on congenic surface markers (CD45.1/CD45.2) by flow cytometer. Gene expression was measured by RNA-seq.

LCMV Infection

WT and *Tbx21*^{-/-} mice were infected either with 2×10^5 plaque-forming units (PFU) of LCMV Armstrong intraperitoneally or 2×10^6 PFU of LCMV Clone 13 intravenously. Eight and 7 days after inoculation, splenocytes were harvested and CD4⁺CD62L^{lo} CD44^{hi} memory T helper cell population was sorted by flow cytometer.

QUANTIFICATION AND STATISTICAL ANALYSIS

RNA-Seq Analysis

We aligned sequence reads from each RNA-seq library to the mouse genome (build mm10) using STAR (v2.4.2a, options: --outFilterIntronMotifs RemoveNoncanonicalUnannotated --outFilterType BySJout) (Dobin et al., 2013), guided by annotated transcript structures (cDNA sequences from ENSEMBL release 82 GRCh38) (Yates et al., 2016). We visualized these alignments by counting positional coverage across the genome (BEDTOOLS v2.15: genomeCoverageBed -split -bg) (Quinlan and Hall, 2010), scaling to 10M total read depth, converting to bigWig (wigToBigWig) (Kent et al., 2010), and viewing in IGV (Thorvaldsdóttir et al., 2013). To quantify transcript abundance we pseudo-aligned RNA-seq reads to ENSEMBL transcripts, using kallisto (v0.42.4, options: -b 50 --single -l 200 -s 30) (Bray et al., 2016). Finally, we identified differentially expressed transcripts using the sleuth R package (Pimentel et al., 2016). In addition to a sleuth q-value < 0.05, we also required differentially expressed genes to have a fold change > 1.5 and expression > 10 TPM in at least one condition.

We quantified the similarity between pairs of expression profiles by calculating the Pearson correlation between log-transformed transcript abundance: $\log_2(1 + \text{TPM})$, considering only genes that were expressed at least 10 TPM in at least 1 sample. We visualized these similarities by creating heatmaps with hierarchically clustered rows and columns (pheatmap R package; <https://cran.r-project.org/package=pheatmap>).

Evaluating Functional Enrichment

We identified GO terms enriched in sets of differentially expressed genes against a background of all expressed genes (at least 10 TPM in either condition) using the GOSTATS R package (options: conditional flag, p value cutoff of 0.001) (Falcon and Gentleman, 2007).

ChIP-Seq Analysis

We aligned ChIP-seq reads to the mouse genome (build mm10) with Bowtie (v1.1.2, options -m 1) (Langmead et al., 2009), allowing only uniquely aligning reads. We then identified peaks using MACS (v1.4.3; default p value threshold of $1E-5$) (Zhang et al., 2008) and GEM (v2.6; options: --k_min 6 --k_max 15) (Guo et al., 2012). We visualized each ChIP-seq dataset by counting positional coverage across the genome (BEDTOOLS v2.24; options: genomeCoverageBed -split -bg) (Quinlan and Hall, 2010), scaling to 10M total read

depth, converting to bigWig (wigToBigWig) (Kent et al., 2010), and viewing in IGV (Thorvaldsdóttir et al., 2013). For gene-centric analyses, ChIP-seq peaks were assigned to the nearest ENSEMBL gene (release 82, GRCh38) within 50 kb using BEDTOOLS (program: closest).

We retrieved published ChIP-seq data to analyze transcription factor binding near repressive and activating T-bet targets (Table S3). Published peak calls were available for all ChIP-seq samples except for IRF7 (Cohen et al., 2014) which we analyzed using the analysis procedure described above. We quantified whether each TF bound more frequently near genes that were repressed than activated by T-bet by calculating the following bias score:

$$\text{repressive bias} = \frac{([\text{no. of T-bet-repressed genes near TF peaks}] / [\text{no. of T-bet-repressed genes}])}{([\text{no. of T-bet-activated genes near TF peaks}] / [\text{no. of T-bet-activated genes}])}$$

We then used a permutation test to evaluate the significance of each observed bias score. Specifically, we randomized the “activated” and “repressed” labels of T-bet-regulated genes 10,000 times (maintaining the total number of each kind) and recomputed the bias score for each TF (holding their ChIP-seq peaks constant). We used this background distribution to compute an empirical p value for the observed bias score, by counting how many background samples had bias scores greater or equal to the actual score, and dividing by the total number of permutations: $(1 + \text{no. of background samples with bias} \geq \text{observed bias}) / (1 + \text{no. of permutations})$. As we used 10,000 permutations, this procedure estimated significance down to a p value $< 1E-4$. For visualization, we summarized the background distribution using the median and 95% confidence interval (Figure 3E).

DATA AND SOFTWARE AVAILABILITY

Raw and analyzed data reported in this paper are available under accession number GEO: GSE96724.